B-spline expansion of scattering equations for ionization of atomic hydrogen by antiproton impact

J. Azuma, N. Toshima, and K. Hino
Institute of Materials Science, University of Tsukuba, Ibaraki 305-8573, Japan

A. Igarashi
Faculty of Engineering, Miyazaki University, Miyazaki 889-2192, Japan

(Received 2 July 2001; published 13 November 2001)

We study ionization processes of atomic hydrogen by antiproton impact in the energy range of 0.1–500 keV by the close-coupling method based on the *B*-spline expansion. Superposition of piecewise *B*-spline functions enables us to express the continuum wave functions more flexibly than the traditional pseudostate representation, in which overall functions such as the Sturmian are used for the expansion. The present expansion also remedies the defect of the traditional one-center expansion that the ionization cross section is underestimated at low energies owing to the finite range of the pseudostates. Our ionization cross sections agree excellently with recent two-center calculations at all the energies. The electron probability densities are also presented in both the coordinate and the momentum spaces.

DOI: 10.1103/PhysRevA.64.062704 PACS number(s): 34.50.Fa

I. INTRODUCTION

The representation of continuum states is a key issue when we deal with ionization processes by the close-coupling method. Discretization of the continuous energy eigenvalues is necessary to accommodate the infinite number of states to the finite-basis-set expansion. For the problems of ion-atom collisions, the pseudocontinuum states, which are square-integrable functions represented as superposition of the Slater or the Gaussian orbitals, have been used traditionally. As both the projectile and the target can support bound states, the two-center expansion is inevitable in this case. Difficulties arise in the interpretation of transition probabilities if we use continuum states with infinite range in the two-center expansions since they have finite overlaps with bound states even at infinite separation. There has not been achieved satisfactory agreement between measurements and theoretical calculations even for the simplest case of the proton on hydrogen-atom collisions [1,2].

The collision of a hydrogen atom with an antiproton is often contrasted with the collision with a proton as an example of charge asymmetry [3,4], similarly to the comparison between electron and positron scatterings with a hydrogen atom. Because the Born cross sections for excitation and ionization of hydrogen atoms are independent of the charge sign of the projectile, the cross sections are expected to be equal for proton and antiproton impacts at high energies. As the collision energy decreases, asymmetry shows up gradually between the two scatterings. The negative charge of the antiproton shields the attractive interaction between the target nucleus and the electron and hence the ionization probability by the antiproton impact becomes larger than by the proton impact at low energies. Another factor that brings about asymmetry to the scattering is that the competing channel of the electron capture is totally absent for the antiproton collisions.

Most of theoretical calculations of the low-energy ionization cross sections of hydrogen atoms by antiprotons are based on the close-coupling method in the semiclassical impact-parameter representation. Since the antiproton does not have a bound state of an electron, the one-center expansion has been used widely. The most standard procedure among them is the expansion of the scattering wave functions in terms of the atomic-orbital (AO) pseudostates [5–7]. Owing to the recent progress of high-speed computers, the number of states for the expansion has been increased up to a satisfactory level that enables the results to be compared with more elaborate calculations. Pons proposed a new expansion designed for the treatment of ionization processes [8]: the spherical Bessel functions, which are the radial part of the wave functions of the plane waves, are used for the expansion. The total scattering system is confined in a finite sphere in order to discretize the continuous spectra.

Wells *et al.* solved the Schrödinger equation directly on a three-dimensional lattice without usage of the basis-set expansion [9]. This approach is called a direct-solution method. Since the finite-difference representation of the wave function on the lattice points is based on the polynomial interpolation, the method can be regarded as an expansion in terms of local polynomials.

Another semiclassical approach not relying on the traditional impact-parameter method was developed by Sakimoto [10,11]. The angular part of the heavy-particle motion is coupled with the electronic motion quantum mechanically and only the radial part is solved classically. The merit of this method is that the assumption of the rectilinear path is not required for the heavy-particle motion. The discrete-variable representation (DVR) employed in this study is an intermediate theory of the direct-solution method and the traditional basis-set expansion. The space mesh is chosen as the zero points of an orthogonal polynomial and the relevant Gauss quadruture is utilized for the integration. The wave functions are expanded in terms of the set of the orthogonal polynomials used for generating the mesh points.

Recently detailed two-center AO close-coupling calculations [12] were carried out for the ionization process to investigate the convergence behavior of the one-center AO expansion. It has been known that the convergence of the one-

center expansion is sometimes slow and confirmation of the convergence within the one-center expansion framework itself is not easy [1]. It was shown in the paper [12] that the one-center pseudostate expansion underestimates the ionization cross sections below 1 keV owing to its inability to represent the expanding distribution of ionized electrons. In this article we denote by ''pseudostates'' those square-integrable functions composed of the Slater or the Gaussian orbitals that decrease exponentially in an asymptotic region. In the intermediate energy region above 1 keV, there still remains a two-center effect that the electron tends to be evacuated near the antiproton by the repulsive interaction from the negatively charged nucleus though this effect does not show up distinctly in the total ionization cross section.

In the present study, we expand the scattering wave functions in terms of the *B*-spline functions centered on the target. The *B* splines have been used widely in atomic physics and many successful applications are reported in the literature [13]. The *B* spline $B_i^k(r)$ is a polynomial of degree $k-1$ extending over k sectors. It takes a different form in each sector but the value and some derivatives are continuous at the sector boundaries. Expressing the wave function as a superposition of those piecewise basis functions we can depict the fine structures of the electron distribution near the antiproton more flexibly than employing overall functions such as the Sturmian or the spherical Bessel functions. Sidky and Lin [14] used the *B* splines for the two-center expansion in the momentum space recently. They calculated the electron distribution during the collisions but the total ionization cross sections have not been reported yet. Our study is complementary to theirs in the sense that our wave functions are expanded in the coordinate space and the basis functions are centered on the target only. Atomic units are used throughout unless otherwise stated explicitly.

II. THEORY

The relative motion of the heavy particles are described classically by a rectilinear trajectory along the z axis with a constant velocity v in the impact-parameter representation. We solve the time-dependent Schrödinger equation of a hydrogen atom interacting with an antiproton.

$$[H_0+H_{int}(t)]\Psi(\mathbf{r},t)=i\frac{\partial}{\partial t}\Psi(\mathbf{r},t), \tag{1}$$

where $\mathbf{r}$ is the position vector of the electron. The atomic Hamiltonian is defined as

$$H_0=-\frac{1}{2}\nabla^2-\frac{Z_t}{r}, \tag{2}$$

where Z_t is the target nuclear charge. $H_{int}(t)$ is the time-dependent interaction between the electron and the projectile,

$$H_{int}(t)=-\frac{Z_p}{|\mathbf{r}-\mathbf{R}(t)|}, \tag{3}$$

where Z_p is the projectile charge. The impact-parameter vector $\mathbf{b}$ is along the x axis and $\mathbf{R}=\mathbf{b}+\mathbf{v}t$ is the internuclear vector. Since the total Hamiltonian $H_0+H_{int}(t)$ is symmetric under the reflection $y\leftrightarrow -y$, the wave function has a definite parity for this reflection. When the initial state has a positive parity like the ground state, $\Psi(\mathbf{r},t)$ can be expanded as

$$\Psi(\mathbf{r},t)=\sum_{jlm} c_{jlm}(t)\,\phi_{jlm}(\mathbf{r}), \tag{4}$$

$$\phi_{jlm}(\vec{r})=\frac{1}{\sqrt{2(1+\delta_{m0})}}f_{jl}(r)[Y_{lm}(\hat{r})+Y^*_{lm}(\hat{r})]. \tag{5}$$

We further expand the radial functions $f_{jl}(r)$ in terms of the $(k-1)$th degree *B*-spline functions. We confine the entire space of the electron in a sphere of radius $r=r_{max}$ and divide the range $[0,r_{max}]$ into N_d-1 sectors $(r_1=0,r_2=,\ldots,r_{N_d}=r_{max})$. The radial wave function $f_{jl}(r)$ is then expressed as

$$f_{jl}(r)=\sum_{i=1}^{k+N_d-2} a_{ji}\frac{(1-\exp[-r])^{l+1}}{r}B_i^k(r). \tag{6}$$

The factor $(1-\exp[-r])^{l+1}$ is introduced so that the radial wave functions may satisfy the boundary condition $f_{jl}(r)\propto r^l$ at the origin. The other boundary condition is $f_{jl}(r)=0$ at $r=r_{max}$. The expansion coefficients a_{ji} is determined so as to diagonalize the atomic Hamiltonian H_0,

$$\langle\phi_{j'l'm'}|H_0|\phi_{jlm}\rangle=E_{jl}\delta_{j'j}\delta_{l'l}\delta_{m'm}. \tag{7}$$

Substituting Eq. (6) into Eq. (3) with the transformation of $c_{jlm}(t)\rightarrow c_{jlm}(t)\exp[-iE_{jl}t]$, we obtain the coupled equations

$$i\frac{d}{dt}c_{j'l'm'}(t)=\sum_{jlm}\langle\phi_{j'l'm'}|H_{int}(t)|\phi_{jlm}\rangle c_{jlm}(t)\times\exp[i(E_{j'l'}-E_{jl})t]. \tag{8}$$

The sum of probabilities over the eigenstates with positive energies $(E_{jl}>0)$ gives the ionization probability

$$P_{ion}(b)=\sum_{E_{jl}>0}P_{jlm}(b). \tag{9}$$

The ionization cross section is given by

$$\sigma_{ion}=2\pi\int_0^\infty dbbP_{ion}(b). \tag{10}$$

The absolute square of the wave function $\Psi(\mathbf{r},t)$ gives the density of electrons in a coordinate space. We integrate the density along the y axis perpendicular to the collision plane,

$$\rho(x,z,t)=\int_{-\infty}^{+\infty}dy|\Psi(\mathbf{r},t)|^2. \tag{11}$$

We also calculate the density in a momentum space

TABLE I. Convergence behavior of ionization cross sections in units of 10^{-16} cm^2 for the three basis sets of the angular part, $l_{max}=3$, $l_{max}=5$, and $l_{max}=8$ at the impact energies, 0.5, 20, and 100 keV.

E (keV)	$l_{max}=3$	$l_{max}=5$	$l_{max}=8$
0.5	1.06	1.07	1.10
20	1.42	1.40	1.41
100	0.984	0.988	0.997

$$\tilde{\rho}(p_x,p_z,t)=\int_{-\infty}^{+\infty}dp_y|\tilde{\Psi}(\mathbf{p},t)|^2, \tag{12}$$

where $\tilde{\Psi}(\mathbf{p},t)$ is the Fourier transform of $\Psi(\mathbf{r},t)$.

III. RESULTS AND DISCUSSION

The matrix elements of the coupled equations are calculated by the Gauss-Legendre quadruture. Except near the origin, the radial part of the wave function is represented as polynomials and the Gauss quadruture gives highly accurate values even for the Coulomb-potential matrix elements. Pons [8] showed that ionization processes of atomic hydrogen by antiproton impact occurs mainly in the region of $|vt|\leqslant 20$. We integrate the coupled equations (8) in the interval $|vt|\leqslant 50$, which is large enough to get converged probabilities. The parameters of the *B*-spline functions are chosen as $k=8$ and $r_{max}=200$. We divided the whole region $[0,r_{max}]$ into 39 sectors enlarging the widths of them for larger r. Overlapping knots are chosen at the boundaries for generating *B*-spline functions and thus 46 *B*-spline functions are used in total. Three different sets are chosen for the angular part to investigate the convergence of ionization cross sections and electronic densities; (a) 460 states with $l_{max}=3$, (b) 966 states with $l_{max}=5$, and (c) 1104 states with $l_{max}=8$. Negative-energy eigenvalues of the hydrogenic Hamiltonian after diagonalization are very close to the exact energies for $n\leqslant 10$. In the calculation of set (c), we coupled only the states with $|m|\leqslant 2$ making use of the dominance of small magnetic-quantum-number states [7].

Table I shows convergence behavior of the ionization cross sections at the incident energies $E=0.5$, 20, and 100 keV. The cross sections agree with one another within a few percent and hence we can conclude that the convergence of the basis functions for the angular part is satisfactory, at least, for the total ionization cross sections. Table II gives the partial-ionization probabilities P_{ion}^{l} at the same energies and $b=1.0$. The contribution of high-angular-momentum states with $l\geqslant 4$ is not negligibly small. Though total probabilities summed over l do not differ very much, the electron distribution is influenced by the contribution of high-angular-momentum components. We employ the set (c) throughout for the calculations of the ionization cross sections.

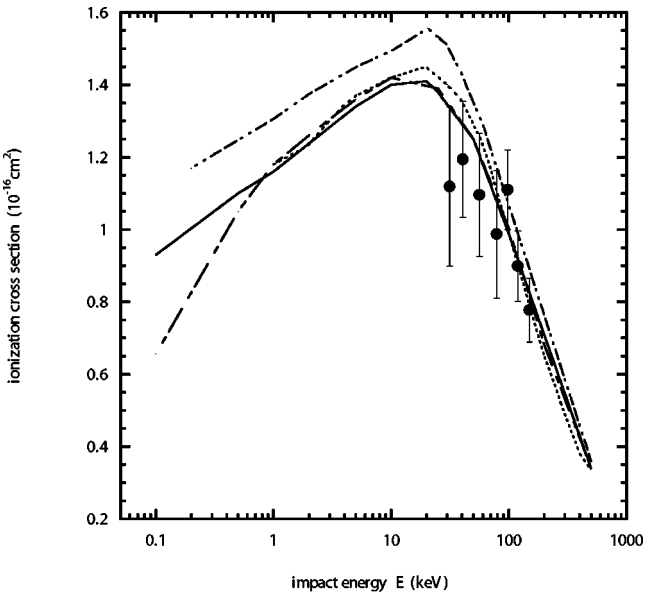

FIG. 1. Ionization cross sections of atomic hydrogen by antiproton impact. The solid line represents *B*-spline expansion; dotted line, spherical Bessel expansion [8]; dot-dashed line, Sturmian expansion [7,12]; two-dots-dashed line, lattice disretization [9]. Experimental data are from Knudsen *et al.* [15].

Figure 1 compares the present ionization cross sections with the other one-center expansions [7,8,12] and the lattice discretization [9], both of which are based on the impact-parameter method with a straight-line trajectory. Above 1 keV our cross sections agree with those of the other one-center expansions. In particular, the cross sections of the Sturmian expansion [7,12] is very close to ours. Though the

TABLE II. Partial-ionization probabilities for $E=0.5$, 20, and 100 keV and $b=1.0$.

E (keV)	l_{max}	$l=0$	$l=1$	$l=2$	$l=3$	$l=4$	$l=5$	$l=6$	$l=7$	$l=8$
0.5	3	0.0331	0.117	0.151	0.182					
	5	0.0565	0.0805	0.129	0.0927	0.0685	0.0582			
	8	0.0474	0.0751	0.116	0.0977	0.0584	0.0495	0.0109	0.0193	0.0228
20	3	0.0109	0.118	0.105	0.120					
	5	0.00948	0.113	0.114	0.0601	0.0336	0.0210			
	8	0.00984	0.112	0.113	0.0640	0.0303	0.0129	0.00534	0.00218	0.00101
100	3	0.0112	0.0848	0.0509	0.0398					
	5	0.0117	0.0887	0.0431	0.0198	0.0121	0.00864			
	8	0.0115	0.0887	0.0453	0.0208	0.00968	0.00447	0.00218	0.00117	0.000724

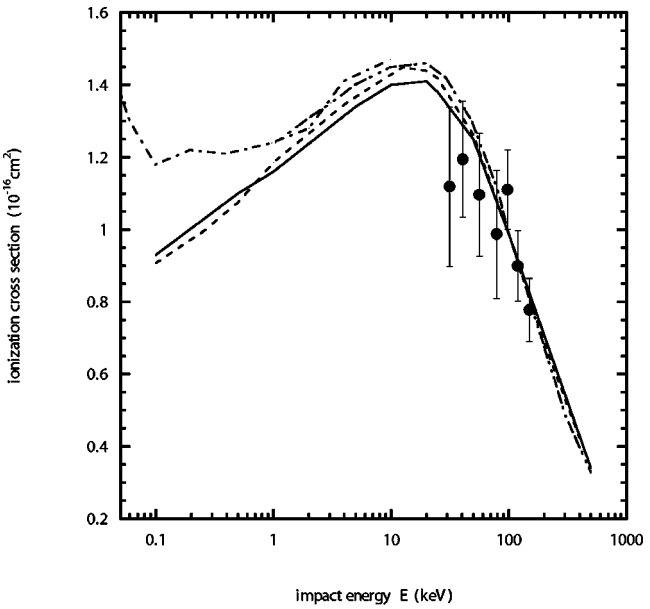

FIG. 2. Ionization cross sections of atomic hydrogen by antiproton impact. The solid line presents *B*-spline expansion; short-dashed line, two-center AO expansion [12]; dot-dashed line, Chebysev-base DVR [10]; two-dots-dashed line, Laguerre-base DVR [11]. Experimental data are from Knudsen *et al.* [15].

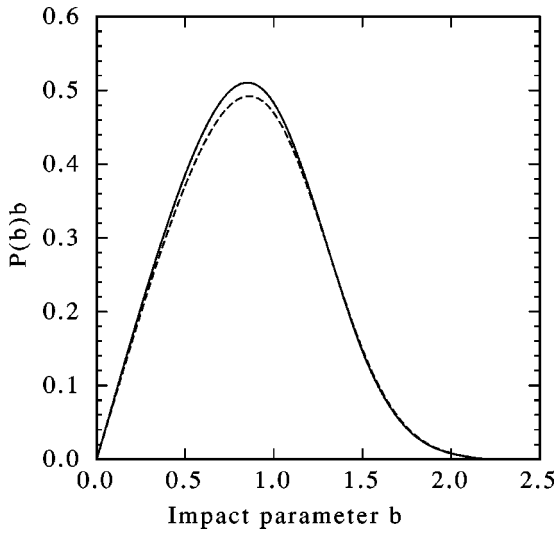

FIG. 3. Ionization probability as a function of the impact parameter *b*. The solid line presents *B*-spline expansion; dashed line, two-center AO expansion [12].

assumption of the straight-line trajectory may become unreliable below 1 keV, we extended the calculations down to 0.1 keV in order to see the dependence on the basis functions within the same approximation. The cross sections of the Sturmian expansion tend to disagree with ours as the energy decreases. As stated in the paper of Toshima [12], the one-center pseudostate expansions, regardless of whether they are Slater or Gaussian, underestimate the ionization cross sections below 1 keV because of the inability of representing diffuse electron distributions spreading out of the range of the basis functions. If one uses smaller exponent parameters for the basis functions, the representation of the diffuse electron distribution is improved to some extent but the increase of the state density after diagonalization enlarges the number of necessary coupled states and the numerical integration of the coupled equations becomes difficult. The cross sections of the lattice discretization are generally about 15% larger than the other theoretical values below 50 keV. They calculated the ionization probability subtracting the bound-state contribution of $n \leqslant 3$ from unity. The contamination of higher bound states with $n \geqslant 4$ into the ionization channel can be one of the reasons for their disagreement with ours. Besides they confined the whole scattering system into a relatively small box introducing an absorbing potential in order to avoid the reflection of the electron clouds at the boundary.

Figure 2 shows comparison with other theoretical cross sections. The present cross sections agree well with the two-center AO close-coupling calculations [12] over the whole energy range presented here. The pseudocontinuum states on the projectile can represent the spreading electron cloud even though the range of the pseudostates is smaller than the radius of the electron cloud. Sakimoto [10,11] used two types of basis functions, the Chebyshev and the Laguerre polynomials, in the DVR method. Both the representations give consistent ionization cross sections but the values are a little larger than ours around the peak position of the cross sections. Below 1 keV his cross sections tend to increase again for decreasing energy. One reason is the curved-trajectory effect caused by the attractive interaction between the proton and the antiproton. The cross sections based on the Chebyshev expansion show some instability below 10 keV as a function of energy. No other theoretical calculations show the undulating energy dependence. It is necessary to remove the numerical instability before discussing the curved-trajectory effect quantitatively.

Figure 3 compares the present ionization probability with that of the two-center AO close-coupling calculations at $E = 0.1$ keV. Since the transition probability as a function of the impact parameter carries more detailed information than the integrated cross section, the good agreement with the two-center AO calculations implies that the calculations converge well within the approximation of the rectilinear trajectory.

The time evolution of the electron densities in the coordinate space are shown as three-dimensional and contour plots in Fig. 4 for $E = 25$ keV and $b = 2.5$. The antiproton is approaching along the z axis. At $vt = 5$ and 10 we can identify a broad dip near the antiproton position, which cannot be produced distinctly by the other one-center calculations [8,12]. At $vt = 20$, where the collision can be thought to having finished, the electron cloud extends up to $r = 30$, which is small enough for the AO pseudostates to express the distribution. Figure 5 gives the densities in the momentum space for the same parameters but the bound-state components are removed to see only the ejected-electron distribution. Before the projectile comes into the electron cloud, the p waves are dominantly excited owing to the long-range nature of the

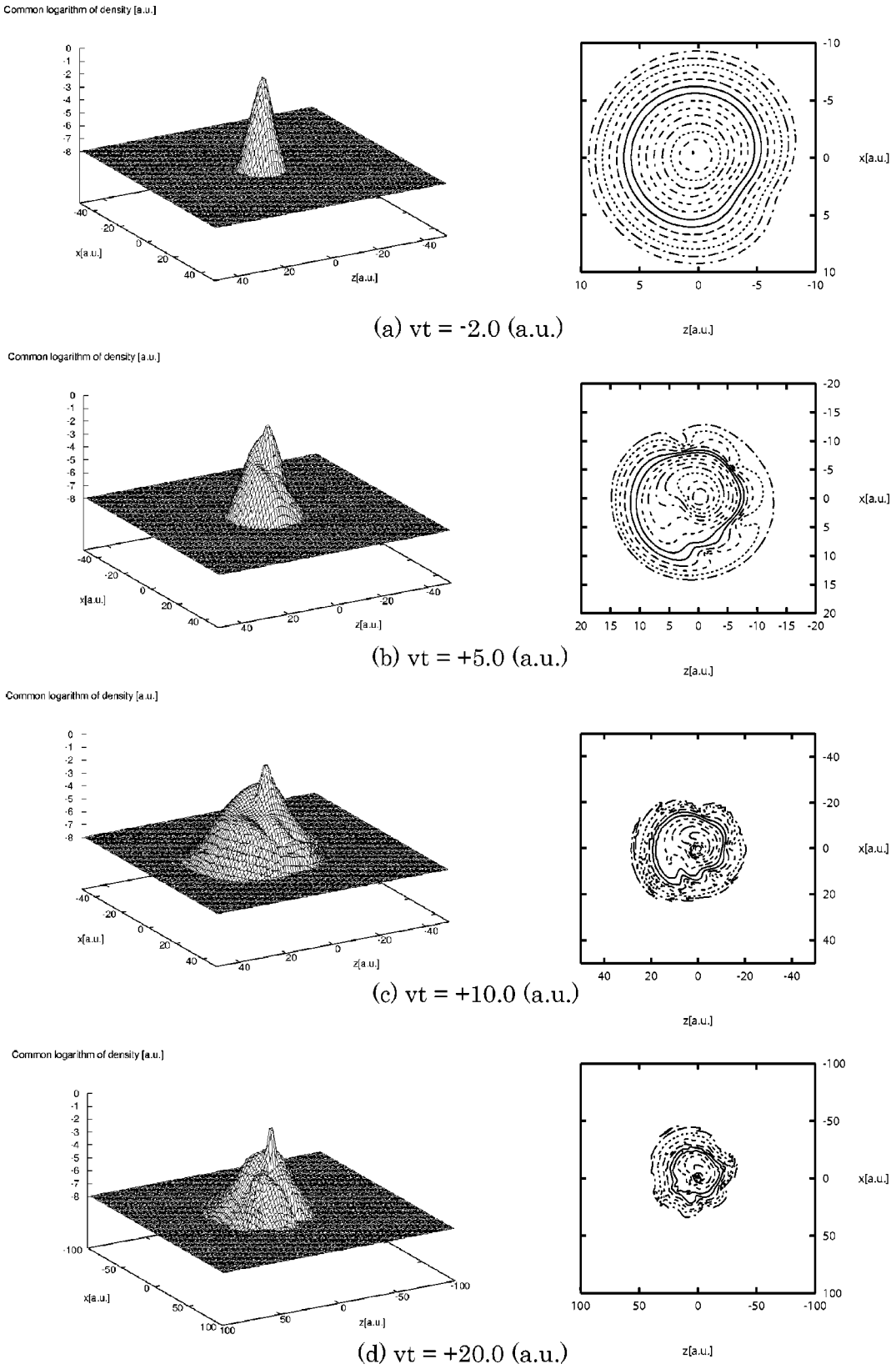

FIG. 4. Time evolution of electron densities in the coordinate space at four positions (a) $vt=-2$, (b) $vt=5$, (c) $vt=10$, and (d) $vt=20$ for $E=25$ keV and $b=2.5$. The left figures are three-dimensional plots and the right ones are contour plots of the same distributions.

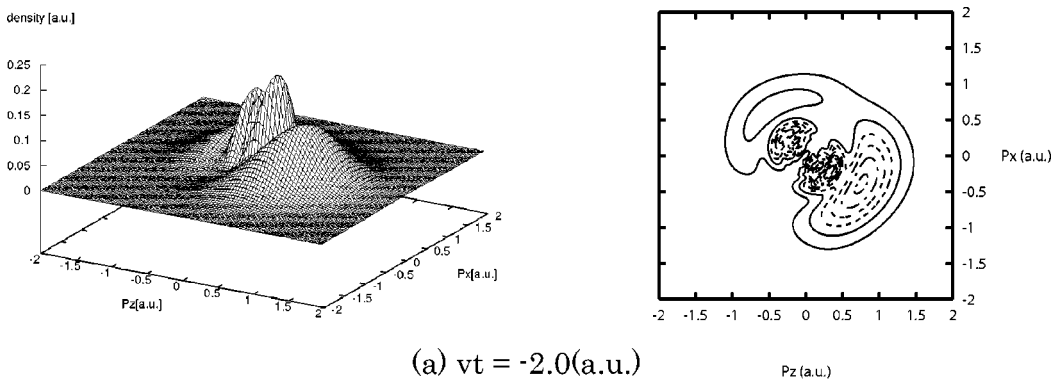

(a) vt = -2.0(a.u.)

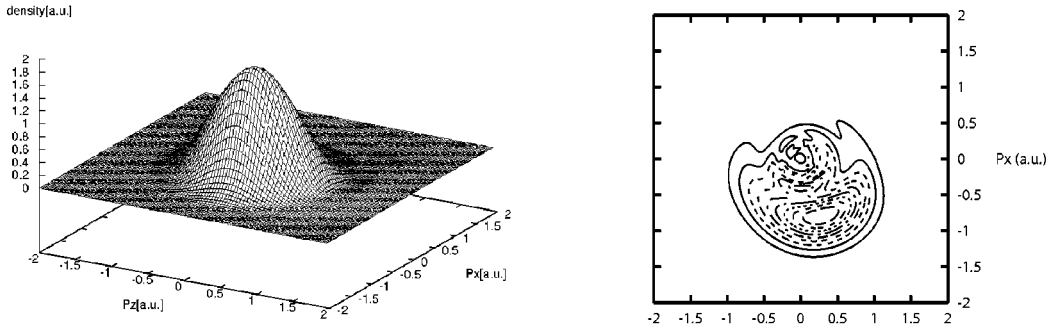

(b) vt = +5.0(a.u.)

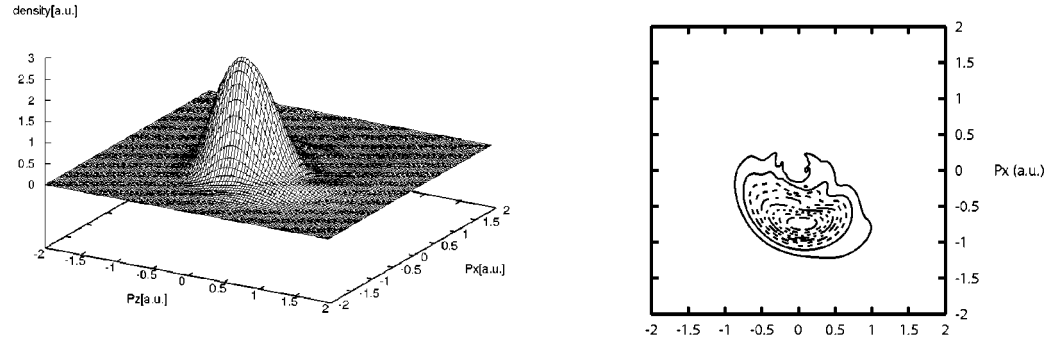

(c) vt = +10.0(a.u.)

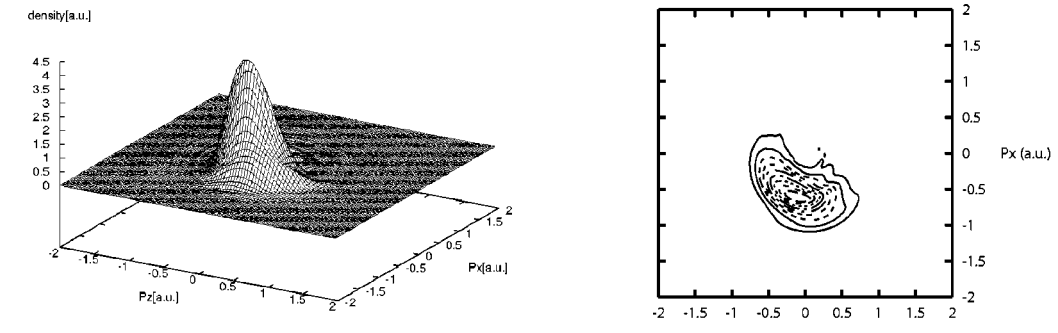

(d) vt = +20.0(a.u.)

FIG. 5. Time evolution of ejected-electron densities in the momentum space. All the parameters are the same as those of Fig. 4 but only the positive energy components (continuum states) are plotted.

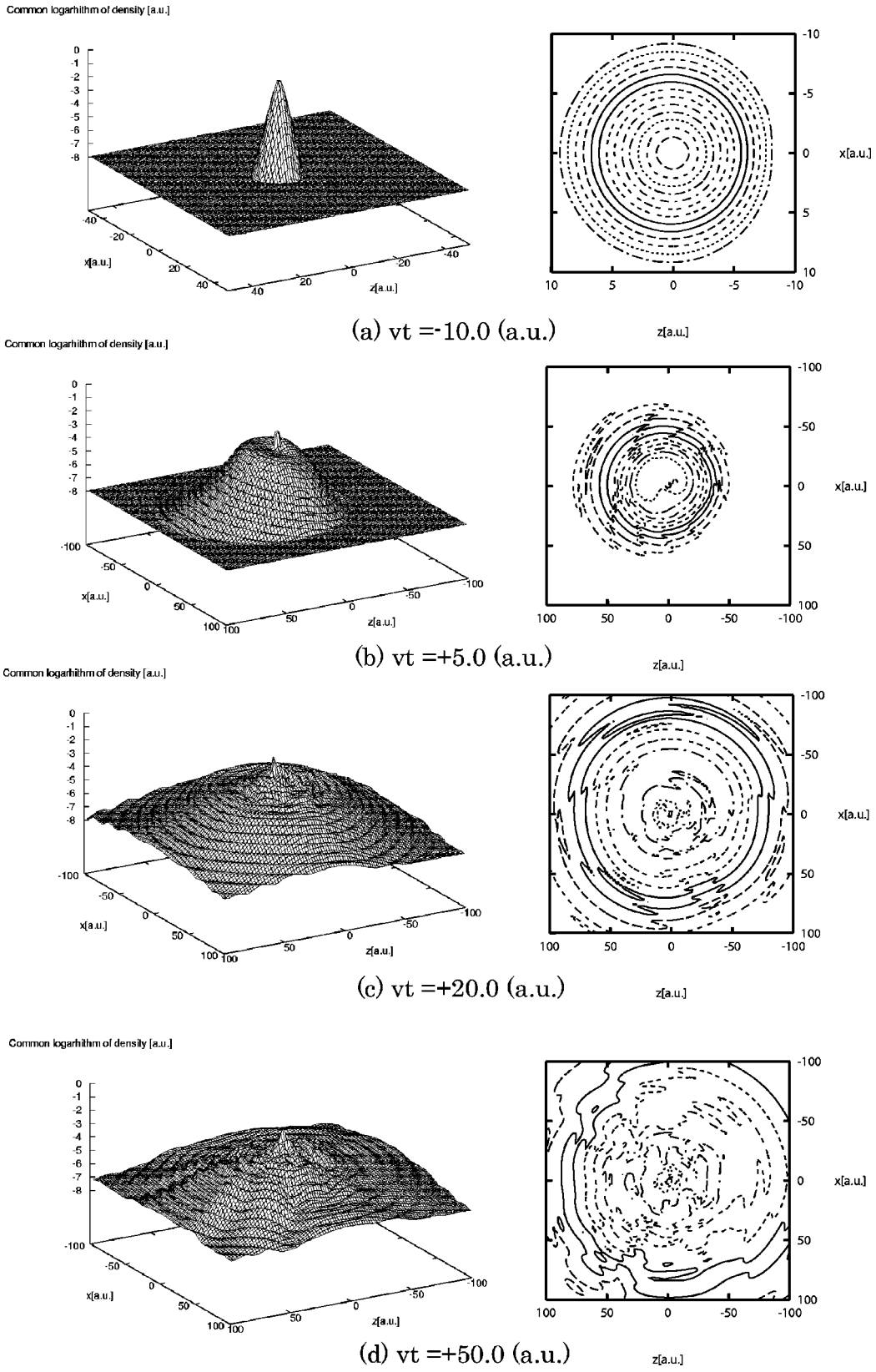

FIG. 6. Time evolution of electron densities in the coordinate space at four positions (a) $vt=-10$, (b) $vt=5$, (c) $vt=20$, and (d) $vt=50$ for $E=0.5$ keV and $b=0.5$. The left figures are three-dimensional plots and the right ones are contour plots of the same distributions.

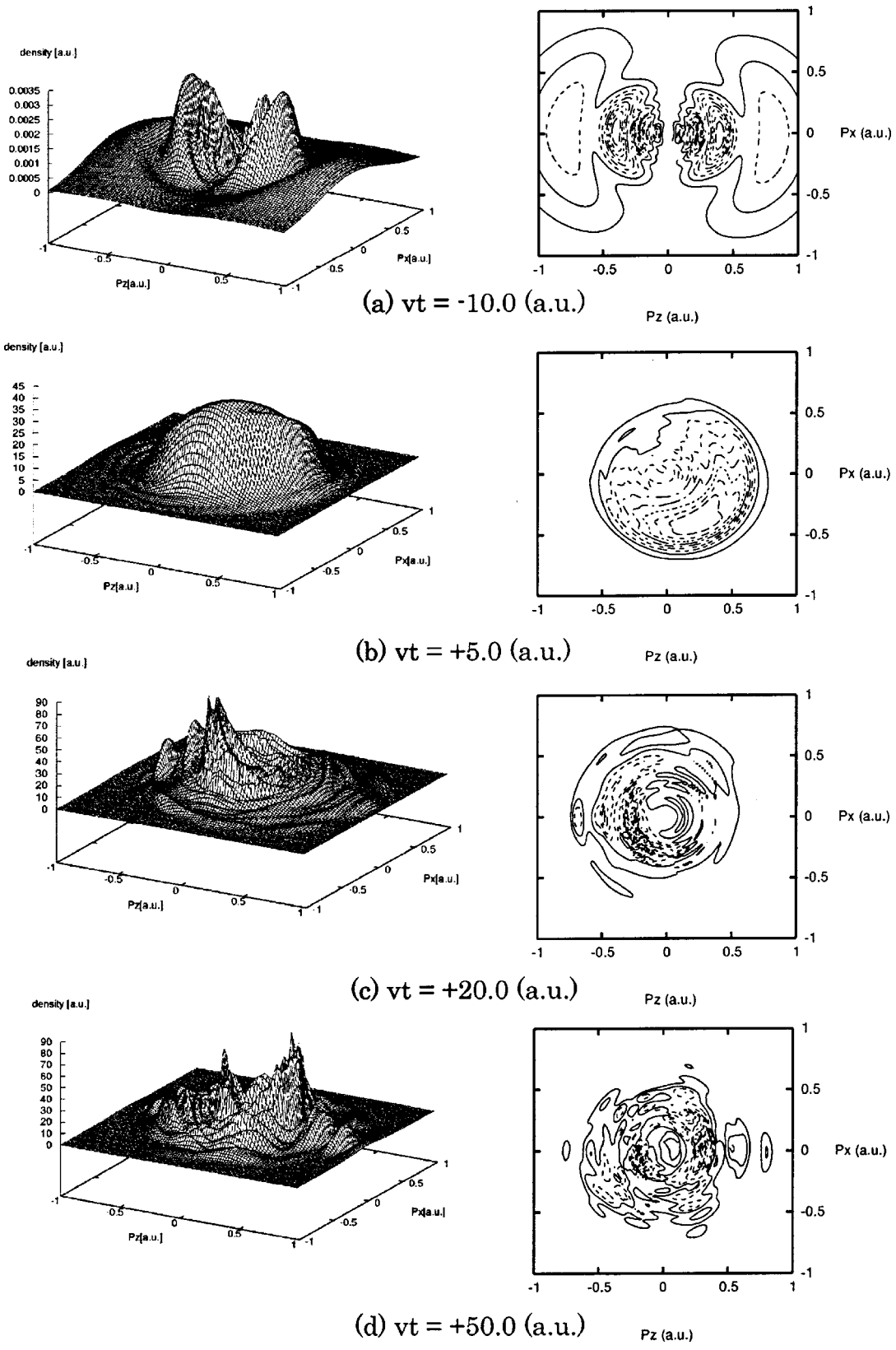

FIG. 7. Time-evolution of ejected-electron densities in the momentum space. All the parameters are the same as those of Fig. 6 but only the positive energy components (continuum states) are plotted.

dipole interaction. We see clearly the *p*-type electron distribution at $vt=-2$. As the antiproton penetrates the electron cloud, the electron tends to be ejected to the negative x direction by the repulsive force. When the collision has finished at $vt=20$, the ejected electrons are mainly scattered to the backward direction, $z<0$ and $x<0$.

Figures 6 and 7 show the density plots for $E=0.5$ keV and $b=0.5$. At this energy the average velocity of the electron is much larger than the antiproton incident velocity. The electron can adjust its distribution to the motion of the antiproton during the collision. At $vt=5$ we see a large dip near the top of the electron clouds, where the electron is evacuated by the repulsive force. At $vt=20$, the electron distribution already extends up to $r=100$ and keeps spreading to the outer region. Evidently the pseudostate one-center expansions fail to describe such diffuse distribution and as a result the ionization cross sections are underestimated. The electron clouds show very complicated structures in both the coordinate and the momentum spaces. Such fine structures of the wave function cannot be represented satisfactorily by the overall functions such as the Sturmian and the Gaussian. The superposition of a large number of piecewise polynomials plays the key role in the present treatment. If one uses overall polynomials, one has to raise the degree up to a large number in order to represent fine structures. As is well known, usage of a high-degree polynomial for fitting data leads to an instability that shows unrealistic undulation among the interpolated points. Spline functions are devised in order to avoid this undesirable feature of the polynomial fitting.

IV. SUMMARY

We have studied ionization processes of atomic hydrogen by antiproton impact by one-center close-coupling calculations using piecewise *B*-spline functions for the expansion. The sphere volume of the scattering system was taken large enough to avoid the reflection of the electron waves at the boundary. Not only the total ionization cross sections but also the electron distribution are calculated in both the coordinate and momentum spaces. At low energies the distributions of the ejected electron show very complicated behavior but the piecewise nature of the *B*-spline expansion can depict such fine structures minutely. The representation of continuum states by the *B*-spline functions proved to be very useful and reliable. Its application to general ion-atom collisions is an interesting extension of the present study.

Above 1 keV, most of existing theoretical calculations agree with one another showing that they are well converged, at least, for the total ionization cross sections. In particular, the present results show good agreement with the recent two-center AO close-coupling calculations in the whole energy range.

At the lowest energy presented in this paper, the trajectory-bending effect due to the attractive interaction between the heavy particles may be important. When the collision energy decreases further and becomes lower than the binding energy of the ground state of the hydrogen atom, ionization can occur only via protonium formation. Purely quantal calculations are required for the consistent treatment of such an extremely low-energy collision.

ACKNOWLEDGMENT

This research was financially supported by a Grant-in-Aid for Scientific Research from the Ministry of Education, Science, Sports and Culture of Japan.

[1] N. Toshima, Phys. Rev. A **59**, 1981 (1999).
[2] A. Kolakowska, M.S. Pindzola, and D.R. Schultz, Phys. Rev. A **59**, 3588 (1999).
[3] A.M. Ermolaev, Phys. Lett. A **149**, 151 (1990).
[4] N. Toshima, Phys. Lett. A **175**, 133 (1993).
[5] G. Schiwietz, Phys. Rev. A **42**, 296 (1990).
[6] K.A. Hall, J.F. Reading, and A.L. Ford, J. Phys. B **29**, 6123 (1996).
[7] A. Igarashi, Phys. Rev. A **61**, 062712 (2000).
[8] B. Pons, Phys. Rev. Lett. **84**, 4569 (2000); Phys. Rev. A **63**, 012704 (2001).
[9] J.C. Wells, D.R. Schultz, P. Gavras, and M.S. Pindzola, Phys. Rev. A **54**, 593 (1996).
[10] K. Sakimoto, J. Phys. B **33**, 3149 (2000).
[11] K. Sakimoto, J. Phys. B **33**, 5165 (2000).
[12] N. Toshima, Phys. Rev. A **64**, 024701 (2001).
[13] F. Martin, J. Phys. B **32**, R197 (1999).
[14] E.Y. Sidky and C.D. Lin, J. Phys. B **31**, 2949 (1999).
[15] H. Knudsen *et al.*, Phys. Rev. Lett. **74**, 4627 (1995).